

EXPRESSION OF PATTERN IN PLANTS: COMBINING MOLECULAR AND CALCULUS-BASED BIOPHYSICAL PARADIGMS¹

PAUL B. GREEN²

Department of Biological Sciences, Stanford University, Stanford, California 94305

Pattern formation in plant meristems occurs across a broad scale. At the topographical level (large scale), tissue folding in the meristem is responsible for the initiation of new organs in specific phyllotactic patterns and also determines organ shape. At the cellular level (small scale), oriented cell division and microtubule-based cellulose reinforcement control cell pattern and growth direction. I argue here that structural specification at each scale is highly efficient if the pertinent gene activity is manifested in two complementary biophysical categories. At large scale, one category is the tendency of the formative tissue to fold with a certain spatial periodicity determined by its material properties (e.g., bending stiffness from cellulose content). This latent tendency is formalized in a differential equation for physical buckling. The second category at this scale comprises boundary conditions that specify how the latent tendency is manifested as topography: whether tissue humps occur as whorls or Fibonacci spirals. This versatile combinatorial format accounts for the relative stability of alternative organ patterning as well as alternative organ shaping (e.g., stamens vs. carpels). It also accounts for the structural shifts seen in normal development and after mutation or chemical/physical intervention. At small scale, the latent differential activity is the tendency for groups of dividing cells to co-align their cytoskeletons. The curvature of the surface opposes this tendency. The least curved part of a new primordium is its quasicylindrical midportion. There, by aligning microtubules and cellulose coherently around the organ, a new growth direction is set. Thus large-scale buckling produces curvature variation, which, in turn, affects the localization and orientation of the cytoskeleton. This scheme for the coherent production of diverse geometrical features, involving calculus at two structural levels, is supported by complex organogenetic responses to simple physical intervention. Also, many morphological alternatives, wild type vs. mutant, reflect single changes in parameters in this differential-integral format.

Key words: biophysics; cell pattern; cellulose reinforcement; cytoskeleton; mechanical buckling; pattern formation; phyllotaxis.

The geometrical features of plants have drawn attention since antiquity on the grounds of their aesthetics and symmetry. Most famous is the crossed spiral or “Fibonacci” pattern seen, for example, in the pine cone and sunflower head. Explaining these patterns, wrote Charles Darwin, could “drive the sanest man mad” (Francis Darwin, 1897). Interest in patterns at the cellular level developed in two ways: (a) it was found that organs, especially in ferns, could arise from prominent apical cells with stereotyped divisions that created the organ’s histology in predictable fashion (Bierhorst, 1971); (b) it was noted that the growth direction of tissue cells was at right angles to the hoop-like reinforcement of their primary walls by cellulose. This alignment is apparently based on

the similar, i.e., transverse, orientation of microtubules in the cytoskeleton (Gunning and Hardham, 1982; Hardham, 1982; Lloyd and Barlow, 1982; Giddings and Staelin, 1991).

Pattern formation in plants clearly spans a wide range of scale. The question arises, how can one best connect this range of phenotypical activity to gene expression as currently understood? Any satisfying explanation must not only account for the details of the geometry and its overall coherence, but must also be compatible with the pertinent developmental biology of production. This article presents a useful causal frame of reference. The tactic is to reduce phenomena at both the genomic and phenotypic ends to the bare essentials and then seek a format to make plausible paradigms connecting them. While the information available is highly fragmented, it is distinctive enough to allow a first effort.

At the phenotypical end, an outstanding feature is the prominence of characters based on angle. Phyllotactic patterns are specified by a divergence angle, the one between organs of successive developmental cycles. The spiral patterns usually have an angle that approximates the Fibonacci angle of $137.51\dots^\circ$ (see below). The divergence angle in whorled patterns is the rotation observed between successive whorls. It is 60° for the iris flower with its nested whorls of three components each.

Angle also enters into the specification of organ identity. When stamens form in snapdragon, they arise as humps in a vertically undulating annulus of formative

¹ Manuscript received 6 December 1998; revision accepted 16 April 1999.

² Paul Green died of cancer before completing the final version of this manuscript. Minor revisions of the text and the figures were done by Jacques Dumais. Correspondence should be sent to Jacques Dumais, Department of Biological Sciences, Stanford University, Stanford, CA 94305.

The family of the late Paul B. Green expresses their gratitude to Jacques Dumais for completing preparation of this manuscript for submission. Jacques Dumais would like to acknowledge the contributions of Mr. Jonathan Fay, Dr. Arif Karabeyoglu, and Dr. Charles Steele. He would also like to thank the numerous colleagues and former students of Paul Green for their comments on earlier versions of this manuscript and Mr. Ted Manning for preparing Figs. 1, 2, 8, and 9. Finally, he is indebted to the Green family for their suggestions and encouragements. Part of this research was supported by NSF grant IBN-9603705.

tissue. When, in the snapdragon mutant *deficiens*, cup-like carpels are produced instead, the annulus of formative tissue undulates in the horizontal plane, thus anticipating the vessel-like nature of carpels. Here a 90° shift in the plane of undulation appears to be an early consequence of mutation.

Angles can be well defined at the cellular level. In the fern *Onoclea*, leaves may have a “two-sided” apical cell, shaped like an orange segment. It makes two ranks of progeny cells at 180°. The shoot of the same plant has a cell that is triangular in surface view. This provides three ranks at 120°. The fact that in many cases the angular correlation is relatively strict, and is inherited, invites explanation. In some other cases, such as stomate formation, the orientation of cell division appears important to later function (Sylvester, Smith, and Freeling, 1996). However, the cell segmentation pattern does not always correlate closely with later differentiation. For example, in the corn mutant *tangled*, relatively normally shaped leaves arise despite considerable variation in division plane alignment and cell shape (Smith, Hake, and Sylvester, 1996). The explanation may be that, despite weak local coherence of cell features, the overall alignment of the reinforcing cellulose across many cells directs growth adequately.

While an explanation for inherited angular features is readily found for structures that self-assemble at the macromolecular level, the connection in higher plants, especially over the size range from microtubule pattern to phyllotaxis, is obscure.

A second challenge at the phenotypical end is the mode of development of the structure of interest. There are several major issues, rarely appreciated. First, some patterns are produced de novo, that is, without any obvious corresponding geometrical antecedents. For example, in dicots, the “featureless” globular embryo normally produces two cotyledons as it becomes heart-shaped. Similarly, in certain flowers, a ring of five sepals arises simultaneously without any (as yet) detected prepattern (Hernández et al., 1991). A second issue is whether the structure is stably propagated, e.g., has a particular divergence angle that varies about some apparent set value. If so, self-correction must be accounted for. Finally, many structural activities occur in alternative forms that are interconvertible. For example, spiral and whorled phyllotactic patterns can each be propagated for many cycles in an apparent self-correcting fashion. Yet within the normal life cycle, or in response to mutation or chemical treatment, whorled apices frequently convert to spirals and vice versa (Meicenheimer, 1981; Mingo-Castel et al., 1984; Kwiatkowska, 1995). Because these diverse perturbations can yield the same response, they likely act at different levels in a common complex pathway.

In sum, for large-scale pattern, there is de novo formation followed by the nonintuitive combination of relative stability and interconvertibility of patterns. A great simplification arises when these three phenomena are interrelated formally. This has apparently been done. Following Turing (1952), it is possible for a formative area to have an intrinsic wavelength, that is, a tendency to undulate (in terms of some chemical or physical variable) where the wavelength, but not the position, is set. For example, fingerprints have the same undulation wave-

length, but the overall patterns made by these undulations are quite distinctive. In de novo formation this wavelength is selectively amplified, from noise, to occupy the available space. Because amplification can be an interactive optimization process (Harrison, 1993), the undulations round off to the nearest whole number (an obvious feature of plant organ pattern). The particular whole number will be a function of the size of the zone and/or the length of undulation being amplified. Once having arisen, this number becomes a boundary condition of the formative area. Thereafter, the pattern is propagated not only because it is an overt feature of the formative area but also because it has the periodicity that is most readily amplified. Different stable whole numbers would characterize different situations depending on boundary conditions. However, large changes could shift the number, despite its relative stability. For example, a size variation could convert a “three-leafed” to a “four-leafed” clover.

To relate such activity to gene expression, schemes are needed where the input comprises reasonable gene products and the output embodies both the geometrical specifics and the various biological modes of implementation. A scheme is developed here that greatly simplifies the structural parameters. Emphasis will be on the two-dimensional geometrical features. Plants are, very roughly, patterns on cylinders. Within this constraint, the phenomenology will be split. Organ pattern and organ shape are change in topography per se (large scale). The cellular level (small scale) deals with issues of alignment: cell files and cellulose reinforcement within the topography. It will be shown that processes at the topographical level appear to affect cytoskeletal activity at the cellular level. Activities at the two levels interact to produce coherence across scales.

To begin analysis, two additional simplifications are made. First is that molecular transductions, while intrinsically complex, can be portrayed as a horizontal Y-shaped symbol (Fig. 1A). The two arms represent inputs of ligand and receptor, of enzyme and substrate, etc. The output, at the end of the stem of the Y, is one of promotion or inhibition of an activity (synthesis, cell growth, assembly of the cytoskeleton, etc.). This symbol is a variation on the usual arrow (\uparrow) or (\downarrow) used in many molecular summary diagrams.

A second major simplification is that a suitable process of regionalization, i.e., designating a generative area, can be taken for granted. Tissues are assumed to have gradients of a chemical sort, or of a physical sort, sufficient to specify an activated formative region with boundaries. The issue reduces to: what happens inside those boundaries to generate the geometrically regular structure seen in plants? I start by examining various established points of view to explain large-scale topography. I consider in sequence three types of mechanism: two emphasize the role of signals, usually mobile molecules, and the third gives the structural responding system a major role.

TOPOGRAPHY I: TWO SIGNAL-BASED MODELS

Interacting multiple monotonic fields—This widely used model embodies the concept of positional information: local activity is prescribed by local conditions in a two-step process (Kalthoff, 1996). The first step is re-

Two Types of Transduction

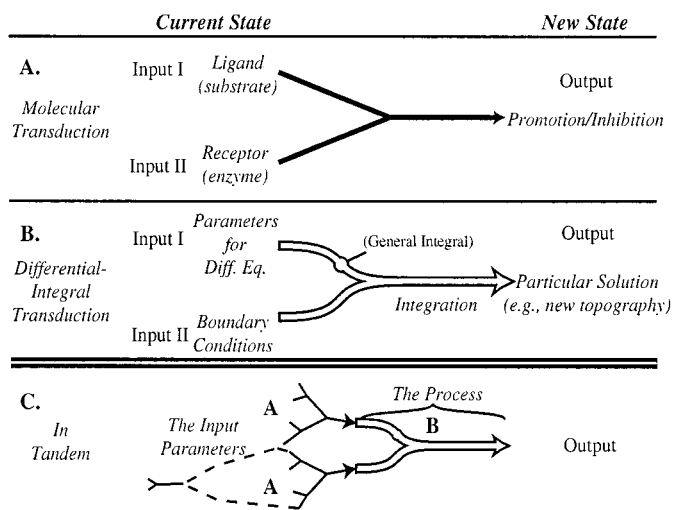


Fig. 1. Two types of transduction or conversion each with two inputs. (A) Molecular steps are simplified to connect two kinds of input with the net result of promotion or inhibition. (B) The input is reduced only to parameters of the differential equation and the boundary conditions. The output is the particular solution to the differential equation. This may take the form of a concentration map if the differential equation describes a chemical process or an elevation map if the differential equation describes the deformation of a solid. (C) The two types of transduction act in tandem. Complex circuitry, including pleiotropic and combinatorial effects, can govern single input terms. In the present view, this activity is a preamble to the pattern-forming process. Differential-integral transduction will be shown to have combinatorial and pleiotropic effects of its own.

gionalization, i.e., the provision of positional information. The diffusion of a signal from a source produces a concentration gradient, a field. Several such fields can interact in combinatorial fashion to subdivide the formative area into ever smaller districts. Progressive subdivision corresponds in many cases to hierarchies of epistatic relationships among mutants (Theißen and Saedler, 1995). The second step constitutes interpretation. Cells have an inherited repertory of responses, physical and chemical, which are evoked by the signals impinging on the cell. Gradients in signals give gradients in cell behavior. These, when summed, constitute tissue behavior. Hence, this format would produce cell pattern, organ shape, and organ pattern by scaling up the same scheme. Cytoskeletal alignment could follow iso-concentration lines, in principle.

Monotonic fields have been invoked for patterning in *Drosophila* where spatial specification in the embryo is sequential and expression patterns clearly anticipate structural periodicity. They have also been applied to bristle pattern formation (Wigglesworth, 1940), a process that is not as well-defined geometrically as plant organ pattern. For plants, this perspective has been the basis of many theories of phyllotaxis where the fields are of inhibition and come from recently made primordia (Mitchison, 1977; Veen and Lindenmayer, 1977; Young, 1978; Chapman and Perry, 1987). This format has been presented as a molecular and cellular basis of plant patterning (Meyerowitz, 1996).

Despite the wide use of this perspective, several aspects do not fit well with the geometrical phenomenology in plants. The following discrepancies justify the consideration of other types of mechanism. (1) This mechanism assumes sequential development, in contrast with the frequent simultaneous appearance of several new organs, e.g., in whorls of developing flowers. Unlike the situation in *Drosophila*, the synchronous physical formation of individual organs does not appear to follow extensive previous internal molecular specification within each. (2) In many of the schemes, particularly the epistatic hierarchies, there is no explicit provision for stability or for de novo pattern formation. (3) When stability is present in phyllotaxis models using monotonic fields, it is usually for the pair of Fibonacci numbers, not the divergence angle (that between successive organs). In nature, the stability is the other way around (Schwabe, 1984). These apparent discrepancies are eliminated when the causal paradigm is changed from one of many interacting monotonic fields to a single undulatory field. Further, the phenomenology of interconvertible related processes is remarkably directly accounted for.

Single undulatory fields—Activities within these fields are modeled by one or more differential equations. The input-output relationship, i.e., converting “before” to “after” for the whole area, is viewed as a single complex transduction (Green, 1996). This is a major feature and will be employed hereafter.

Differential-integral transductions—The basic developmental step is embodied in a diagram, Fig. 1B, which has the form of a curved horizontal Y. One arm is the input for the parameters of the differential equation. The other is for particulars of the boundary conditions. The two inputs meet at the junction where the specific integration takes place. The output, a pattern, is the stem of the Y. Note that the input parameters are derived from previous transductions at the molecular level. These input pathways are often complex and lead to combinatorial and pleiotropic effects. By preceding the patterning process itself, however, they are distinct from it (Fig. 1C). This format apparently meets the criterion that the input categories are biologically plausible and that the output produces spatially periodic pattern.

The undulatory field, already mentioned, has a latent intrinsic wavelength. Wavelength is implicit in one or more differential equations. The developmental transduction, which corresponds to the integration in the model, amplifies this wavelength preferentially. This process constitutes the theme. Because the undulatory pattern must conform to the boundary conditions, integration can both fix the location of the undulations and modify them somewhat. This provides variation. An example is shown in Fig. 2 illustrating two modes of whorl formation.

With certain equations, the integrals are relatively insensitive to small changes in input parameters. Such solutions are called optima. There may be just one, a primary optimum, and/or several secondary optima. An example of the latter is that only whole numbers (no fractions) of undulations arise in a ring despite continuous variation in circumference (see Fig. 3 in Green, Steele, and Rennich, 1996). Each number is a secondary opti-

The Basic Transduction for Buckling

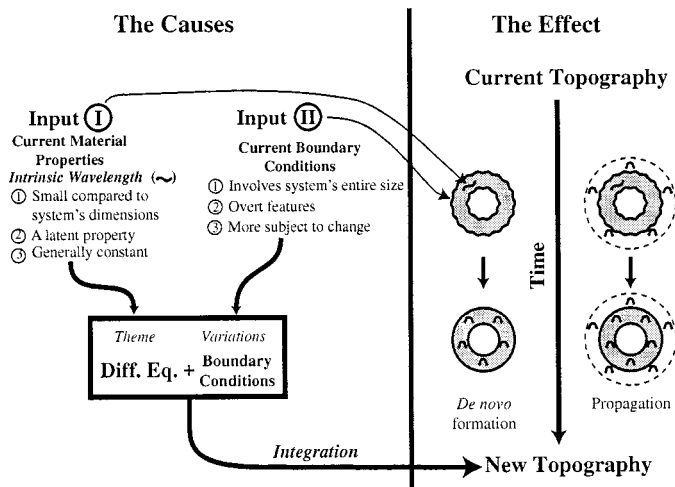


Fig. 2. The basic transduction for buckling: the conversion of one topography to another. For de novo formation this process transcends three levels of structure: tissue, organ, and organ system. For propagation, it simply reiterates a preestablished pattern. Genetic input takes two forms. (I) The input pertaining to the current properties of the system that apply to the differential equation. In this case the main feature is the intrinsic wavelength (the theme). (II) The boundary conditions give details of a particular solution. The resulting integration displays both the consistent general feature (undulation) and distinct variations of its compliance with the boundary conditions.

mum. Larger variations in boundary conditions can bring on major variations in the outcome of the integral, e.g., switching between alternative arrangements or shapes of undulation (Green, Steele, and Rennich, 1996).

A specific undulatory field of signals (reaction-diffusion)—The best known undulatory fields are generated by reaction-diffusion (Turing, 1952). The key inputs for the differential equation are the diffusion constants, the synthesis rates, and the decay rates for two types of morphogen molecule. The intrinsic wavelength can be calculated from these values. At the margins of the pattern-forming area, the boundary conditions are flux and concentration for both morphogens. Integration of the equations provides a dynamic steady-state profile of the concentrations of the diffusing agents. This output is a prepattern, i.e., a contour map of concentration. The patterning process is dynamic and dissipative in that there is turnover of the molecules involved.

The process is very well developed for animal coat patterns (Murray, 1981). It is the uncontested mechanism for sea shell patterning (Meinhardt, 1995). It has been applied extensively to unicellular plants (Harrison et al., 1981; Lacalli, 1981; Holloway and Harrison, 1999), as well as phyllotaxis (Berding, Harbich, and Haken, 1983; Bernasconi, 1994). It has received experimental support through temperature and calcium concentration effects (Harrison et al., 1981; Harrison and Hillier, 1985).

However, reaction-diffusion has several impractical features. The output is not structure, but rather a prepattern for it. Also, the model involves kinetic parameters of generally unknown compounds. Putative values are generally used. There is synthesis and decay, i.e., turn-

over of the pertinent molecules, the cost of which is hard to estimate. It is thus difficult to find an objective criterion, at least an energy-based one, for the pertinence in nature of one patterned solution relative to another. Many of the shortcomings are eliminated if one considers a responding-system model such as mechanical buckling.

TOPOGRAPHY II: A RESPONDING-SYSTEM MODEL (MECHANICAL BUCKLING)

Theory—Pattern and shape formation are treated here as the generation of a specific undulating physical topography. The physical patterning system consists of two material layers, in broad contact. They correspond to the tunica and corpus in plants. While cells are present, and contribute to material properties, the key patterning properties of the system are not contingent on cell behavior. The calculations for the structure to be formed are in terms of continuum mechanics (Szilard, 1974; Green, Steele, and Rennich, 1998).

The major input to the equation consists of two material properties characteristic of solids. These are the flexural rigidity, applying to the tunica, and the elastic constant (for displacement normal to the plane) applying to the corpus. Both parameters are reasonable "downstream" developmental consequences of gene expression. Moreover, they impart the tunica with a tendency to undulate at a specific wavelength. In the simplest case, the intrinsic wavelength is proportional to the fourth root of the quotient of these two properties. Integration gives a three-dimensional configuration (a topography) in static elastic equilibrium. Continuous conversion from an elastic to an irreversible deformed state is assumed (there is "quasi-static" physical equilibrium).

The essence of the differential equation is that in-plane stress is balanced by two opposing tendencies: reluctance to bend and reluctance to displace in the out-of-plane direction. A given imposed stress leads to an equilibrium undulatory configuration. On-off control is through the presence/absence of stress, or through the system having a wavelength larger than the size of the system. Boundary conditions are complex. They specify two of the following variables: deflection, rotation, moment, or shear at each point on the boundary. In the present case, they provide great versatility for configuration change, even from an initially flat surface.

A great advantage of buckling is that it is a minimum energy phenomenon. That means that patterns will spontaneously tend to approximate the minimal energy pattern, a direct self-correction mechanism. By the same token, conversion to a different stable pattern can be the response to a strong perturbation. One way to determine the minimal energy pattern is with the critical stress. This is the level of stress where the structure no longer effectively resists deformation. For configurations close to the minimal energy pattern, the critical stress is small, while for configurations far from it the critical stress is high. The advantage of this approach is that the critical stress can be determined for arbitrary configurations. One can thus predict among a group of configurations which one is closest to the minimal energy pattern: it is the configuration with the lowest critical stress value.

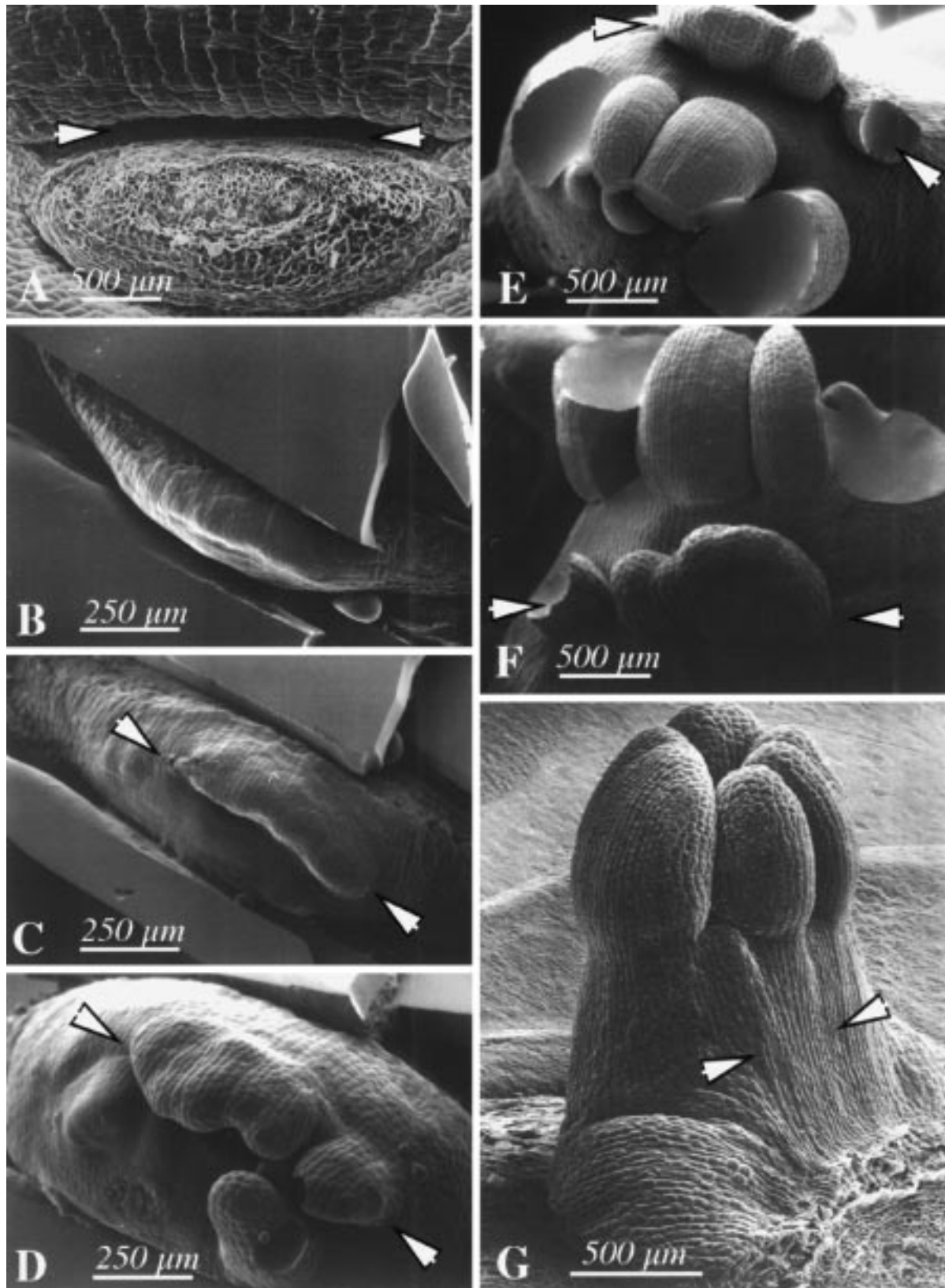


Fig. 3. Physical induction of ectopic leaves on the residual meristem of a detached *Graptopetalum* leaf. (A) The residual meristem is the recessed area above the abscission scar (arrowheads)(photo by K. E. Brooks). In subsequent pictures part of the overarching cells have been removed to facilitate the observation of the meristem. (B–F) Sequential scanning electron micrographs of the same growing plantlet using the replica method. (B) A residual meristem constrained by a frame of glass chips. (C) A precocious and ectopic row of leaves, now a ridge, is forming (arrowheads). (D) The former ridge is now a row of partly fused ectopic leaves. Normal leaves have started to form below and at left. (E) Normal leaves, below, now dominate; older ectopic row is at top. Void areas are simply unfilled replica sites. (F) New normal leaves above, ectopic row below. (G) A typical control plantlet (photo by K. E. Brooks). The ectopic row would be horizontal, at center (arrowheads). The image also illustrates cell patterns, i.e., the origin of the histology of a new primordium. There has been a 90° shift in cell file alignment from the horizontal flank (foreground) to the erect new stem. No shift occurs at the midline of the new stem, at right. This originally disjointed activity results in a uniform file pattern around the new stem. See Fig. 8C.

Experimental evidence—Many observations suggest an organizing role for physics acting at the tissue level. Experimentally, the regional application of the protein expansin, considered to affect only material properties of the cell wall, can bring on de novo organogenesis and also influence phyllotaxis (Fleming et al., 1997). In sunflowers, direct physical intervention, which mechanically constrained the formative area, changed tissue folding patterns in predicted ways. This resulted in changes in organ shape and identity (Hernández and Green, 1993). In a third case, shown here in preliminary fashion, mechanical constraint in the form of a glass frame induced an ectopic row of leaves in an expanding meristem (Fig. 3).

The most direct interpretation for the above is that tissue scale processes, apparently physical, can influence details of subsequent cell behavior and presumably gene expression. Tissue effects may be causes, as well as consequences, of cellular activity. This buckling mechanism retains the many virtues of an intrinsic wavelength such as seen with reaction-diffusion, but here the essential communication is achieved physically. Stress can be viewed as the “prepatterned signal”; it is, however, more directly coupled to the response than conventional mobile signals. In fact, the signal and the response may be regarded as essentially the same process.

Buckling and organ pattern—Patterns in plant meristems can be broadly classified as whorled or spiral (Fig. 4). A whorl consists of a whole number of organs, evenly spaced in a ring. A plant with a whorled pattern has several such rings, with the organs in adjacent rings being staggered or nested. The characteristic divergence angle, that between organs of adjacent whorls, is simply 360° divided by twice the number of organs per whorl (see Fig. 4A). This gives a simple fraction of a circle. Such angles are usually stable in development and in evolution. Dicotyledonous flowers generally have whorls of four or five organs (divergence angle of 45° or 36°); monocot flowers generally have threefold symmetry (divergence angle of 60°). However, the number of organs is subject to control by chemical treatment (Rasmussen, 1991) and genes such as *PALLIDA*, *ABPHYL*, *CYCLOIDIA*. The most common whorled vegetative pattern (decussate), seen in maples and mints, has two leaves per whorl. Many plants, especially grasses and other monocots, have organs placed in a zig-zag fashion, in a plane (distichous phyllotaxis). This is viewed here as a “whorl of one” with a divergence angle of 180° . Whorled patterns in general are radially symmetrical.

The spiral pattern is characterized by two sets of spirals, one steep and one gentle, with opposite handedness. The numbers of spirals in the contrasting sets are most often consecutive numbers in the Fibonacci sequence: 1, 2, 3, 5, 8, 13, The higher number is associated with the steeper spiral. The divergence angle, that between consecutive organs, is generally close to $137.51 \dots^\circ$ (the Fibonacci angle, Fig. 4B). The Fibonacci angle is the value, as n goes to infinity, of the ratio $(F_n/F_{n+1}) 360^\circ$, where F_n is the n^{th} member of the Fibonacci sequence. Other spiral patterns are occasionally seen, but the Fibonacci spirals are by far the most common (Jean, 1994). As a rule, the divergence angle for spiral patterns con-

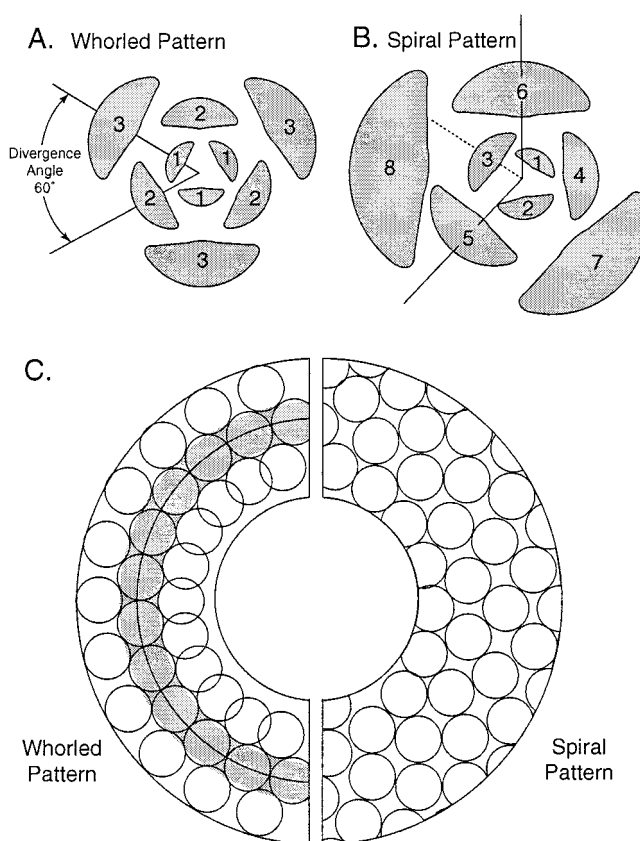


Fig. 4. The close packing of similar disks in polar coordinates. (A) and (B) show placement rules for the whorled and spiral patterns. (C) In an annulus of finite width the packing of nested whorls is possible only in an infinitesimal narrow ring (shaded region). The departure from the optimum is caused by disks toward the interior overlapping and those toward the periphery becoming separated. This would correspond in the case of buckling undulations to a stretching or a shortening of the wavelength. Such a gradient would increase the total energy of the system. For buckling in a hexagonal pattern (nested whorls), energy status is sensitive to annulus breadth. For the Fibonacci spiral pattern, the packing is regular but somewhat less close (or higher energy) than hexagonal. However, this packing arrangement is insensitive to annulus width. Hence narrow annuli will be of less energy (per undulation) if the undulations are in whorls; broad annuli will be of less energy if the undulations are in the spiral pattern. Thus change in a single parameter, annulus width, which is plausibly under biological control, could be the basis for the switch between whorl and spiral patterns.

verges to an irrational number. When the organs are large compared to the annular zone where they are generated, the number of spirals is small. For example, it is often (5, 8) in a pine cone. When the organs are small compared to the annular zone, the numbers are large, e.g. (55, 89) in the sunflower head. This is independent of the divergence angle in contrast to the whorl pattern (Schwabe, 1984).

The production of whorled and spiral patterns requires de novo formation and propagation (Fig. 2). Two approaches were followed in trying to understand the possible role of mechanical buckling in these processes. First, the patterns were simulated in a static fashion. This approach was used to evaluate the energy of a wide range of patterns and to determine under which conditions a given pattern would predominate. The second approach

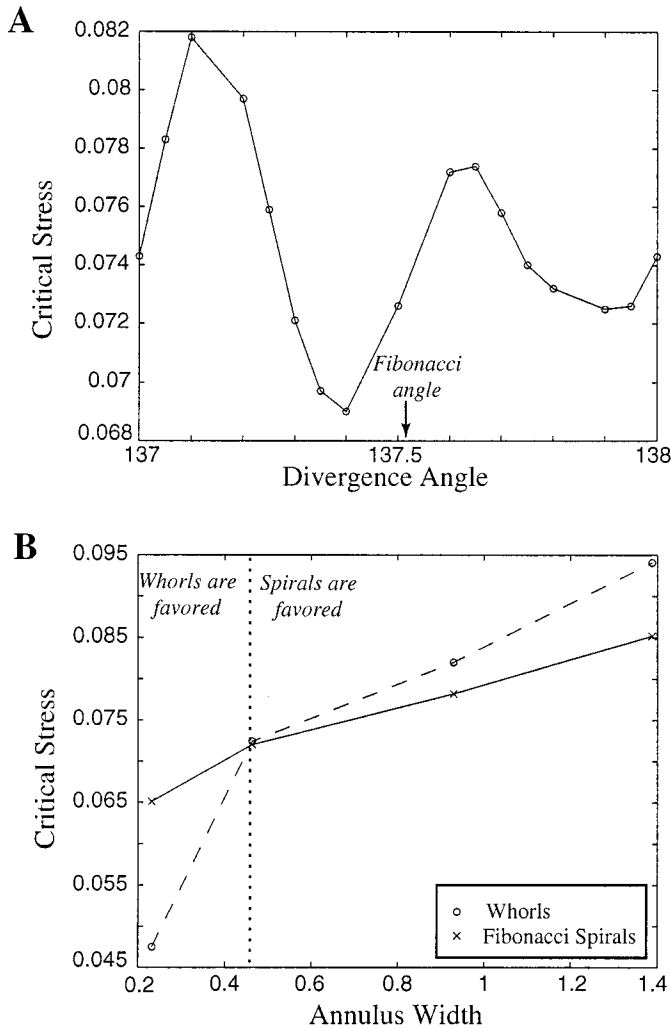


Fig. 5. Energy considerations for static patterns on an annulus. Energy is measured in terms of critical stress value. (A) Spirals: sensitivity to change in divergence angle used in construction of the pattern. Because the patterns used to determine the total energy contain a finite number of undulations, the minimum observed only approximates the Fibonacci angle of 137.51° (arrow). (B) Sensitivity of whorls and spirals to the width of the formative annulus. Note the threshold value for annulus width where the energetics dictate pattern transition. Graphs prepared by Dr. Arif Karabeyoglu (Department of Aeronautics and Astronautics, Stanford University).

was a quasi-static simulation of pattern (i.e., several small static steps in sequence as an approximation of a dynamic process). This was used to examine the stability of the patterns during propagation.

Static simulation of pattern—Mechanical buckling can explain de novo formation of whorls and the common transition between whorls and spirals. A laterally confined flat annulus with an intrinsic wavelength, when caused to expand in-plane will produce a whole number of undulations in a whorled pattern. The fit is to the nearest whole number. When the width of the annulus is one wavelength and the annulus is many wavelengths in circumference, the undulations are humps that are approximately circular in cross section (Green, Steele, and Ren-

nich, 1996). A similar annulus or disk provided with adequate boundary conditions can also produce a spiral pattern (Green, Steele, and Rennich, 1998). However, this is not de novo formation per se since the information for the spirals has to be included in the boundaries.

Transitions between whorls and spirals are common during the vegetative and generative phases of development. Sunflower and snapdragon are good examples of whorls converting to spirals. Spirals convert to whorls during individual flower formation in *Echeveria* and *Silene*. Conversion is controlled by known genes: *LEAFY*, *FLORICAULA*, *MATURA*, etc. Similar switchings are controlled by known hormones (Mingo-Castel et al., 1984; Marc and Hackett, 1991; Lyndon, 1994).

Meicenheimer (1998) has suggested that models of plant phyllotaxis should be able to account for these common transitions. This can be addressed by asking whether there is an energetic basis for the whorl-spiral duality. Because of the minimal energy nature of mechanical buckling, the problem is reduced to finding conditions under which whorled or spiral patterns are minimal energy.

For simplicity, the alternative patterns are portrayed as closely packed circles (Fig. 4C). The correspondence between phyllotactic patterns and those of close-packed circles has long been recognized (van Iterson, 1907; Ridley, 1982; Erickson, 1983). For the surface of a cylinder, the optimal close-packed pattern is the well-known hexagonal array (Tarnai and Gaspar, 1995). For a disk, patterns based on the so-called "cyclotron spiral" represent the optimal close-packed spiral arrangements (see Ridley, 1982). It is clear in Fig. 4 that, for an annulus, the packing of nested whorls is ideal only in an infinitesimal zone (shaded region in Fig. 4C). A broad annulus will be, on average, less regularly packed (hence of higher energy). The spiral pattern is locally less compact than optimally packed whorls, but it is less sensitive to annulus width. The issue is whether there is a width beyond which a spiral packing can be of lower energy than packing of nested whorls. This provides a potential switch for pattern.

To make quantitative energy comparisons of different undulatory patterns on an annulus, it was necessary to generate patterned topography artificially. The appropriate set of points was produced. For the whorled pattern, a fixed number of undulations were simply placed at different radial distance as in Fig. 4C. For the spiral pattern, the position (R) of each element was determined with the following algorithm in polar coordinates:

$$R_n = (n\alpha, \sqrt{nh}), n = 1, 2, 3, \dots$$

where α is a fixed divergence angle (e.g., 137.51°) and h is the radial rise. At each point a radially symmetrical Gaussian function, maximum at the point, was generated. The curved surfaces were summed. The energy of the resulting quasi-sinusoidal topography was then evaluated.

For whorled patterns, the energy per undulation varied only slightly as a function of circumference. Thus annuli with an exact whole number of wavelengths around the circumference were secondary minima. Within these constraints, whorled patterns were minimum energy. As annulus width increased, however, energy values increased rapidly (Fig. 5B).

The Fibonacci pattern is of lower energy compared to nearby configurations that differ in divergence angle, α (Fig. 5A). The energy status for these spiral patterns is relatively insensitive to annulus width. Thus there is a threshold value for annulus width below which whorls are favored and above which spirals are favored (Fig. 5B). In this treatment, the nature of the "switch" between patterns is explicit in terms of continuum mechanics and, potentially, in terms of biological activity. To embody the biological control of annulus width, some non-periodic activator molecule, diffusing from recently made organs, could vary in its range or effectiveness (Hernández et al., 1991). Pertinent genes involved in this could be *LEAFY* and *MATURA*; a pertinent chemical would be gibberellic acid (Rasmussen, 1991).

Quasi-static simulation of pattern—Pattern propagation is generally characterized by a positioning rule that applies throughout propagation. It relates local activity for placing a new structure to features of the pre-existing pattern. For whorled patterns, the rule is that a new organ is placed interior to, and midway between, two organs of the previous generation (Fig. 4A). These organs are identical in size, age, and distance from the center of the array. For spiral patterns, a new organ is also placed relative to two older organs. They are, however, of different previous cycles. Accordingly, they differ in size and in distance from the center. The positioning rule does not use the bisection of an angle (0.5 : 0.5) as with whorls; it rather uses the Golden Section (~0.618:0.382) (Fig. 4B). In both cases the rule is repeated to propagate the pattern.

A major feature of propagation, rarely modeled, is that it is a moving boundary phenomenon. The formative annulus has young undifferentiated tissue at the inner margin, maturing organs at the outer boundary. Organs are forever moving outward relative to the annulus. In the steady state, seen in vegetative growth, the patterning influence continuously acts inwardly to compensate the physical outward motion. The tissue moves through boundaries that are in constant relative position on the parent axis. This reconciles unlimited cycling of the pattern with constant dimensions of the annulus. In a flower, the formative region moves inward across stationary or slowly growing tissue. In this case, the apical dome region becomes fully occupied by organs. In both cases, however, there is relative motion between the boundaries and tissue. A shift between the two types of patterning influence (in place vs. progressive) often occurs at floral induction. The extent of propagation of organ types within flowers is governed by known genes: *SUPERMAN*, *CLAVATA*, etc.

A given propagating pattern can persist through vast numbers of cycles, while varying about a consistent mean divergence angle (Fujita, 1939). This implies strong stability, as does the experimental work of Snow and Snow (1935) showing that a surgically induced spiral development reverted to the original decussate pattern.

To simulate the propagation of whorled and spiral patterns a quasi-static approach was used. An annulus with a width of about one wavelength was given specific boundary conditions. The inner boundary had zero deflection and moment, and the outer one was "clamped"

with a sinusoidal profile characteristic of nested whorls. The whole annulus then was forced to comply, via the buckling equations, to the imposed boundary profile. Propagation was implemented by having development occur in small steps. The inner boundary was moved inward by 10% of annulus width. In-plane stress was applied to amplify the topography. The outer 10% of the annulus was removed from the formative zone. (In an actual plant this topography remains present but no longer affects the patterning occurring in the formative region.) The boundaries were restored to the original dimensions. This cycle was repeated to show that a whorled pattern can be propagated indefinitely.

Moreover, when a departure from the typical pattern (e.g., a truncated undulation) was introduced, prominence of the error diminished. During propagation, interestingly, correction did not take the form of the error being eliminated. Rather, the error simply failed to be amplified by buckling and became relatively less detectable during its movement through the annulus (Fig. 6). Self-correction was thus present. The form of the undulations was not uniform. The solutions to the buckling equations approximate the natural wavelength in the radial direction, but in the circumferential direction wavelength tends to decrease with radius. Thus, within the annulus, the aspect ratio of the undulations is changing.

The propagation of spiral patterns was modeled in a similar fashion. An annulus is given an outer profile, which is a vertical section through a Fibonacci pattern. The annulus topography is made to fit the profile. The quasi-static simulation, above, was applied to propagate the pattern. Propagation was indefinite, but, surprisingly, there was no preference to the Fibonacci angle. All spiral patterns could be made stable by selecting the material properties properly.

Relevance—The buckling simulations have provided a specific explanation for three important phyllotactic features. First, whorls can be produced de novo but not spirals. This could explain in part why de novo pattern formation in plant yields mostly whorls. Second, a condition (i.e., annulus width) favoring the transition between whorled and spiral patterns was found. Finally, conditions could also be selected such that whorled and spiral patterns were propagated indefinitely. However, self-correction was demonstrated only for whorled patterns at this stage. Attention now shifts to the cases where differences in shape between individual primordia are emphasized.

Buckling and organ shape—Initial organ shape correlates with organ identity. I will focus on stamens that become stalk-like and carpels that become cup-like (closed vessels, ultimately). In snapdragon, stamens originate in the third whorl as five vertical undulations in an annulus (Fig. 7A). In the *deficiens* mutation, a comparable annulus undulates horizontally, making a wavy ribbon with five cup-like undulations that become carpels (Fig. 7B). Here the alternatives in organ form appear to reduce to a 90° variation in the plane of undulation.

In the above treatment of organ pattern, the parameters for wavelength varied only in the vertical plane of the undulation. That is, there was an elastic foundation directly below the annulus. The horizontal boundaries were

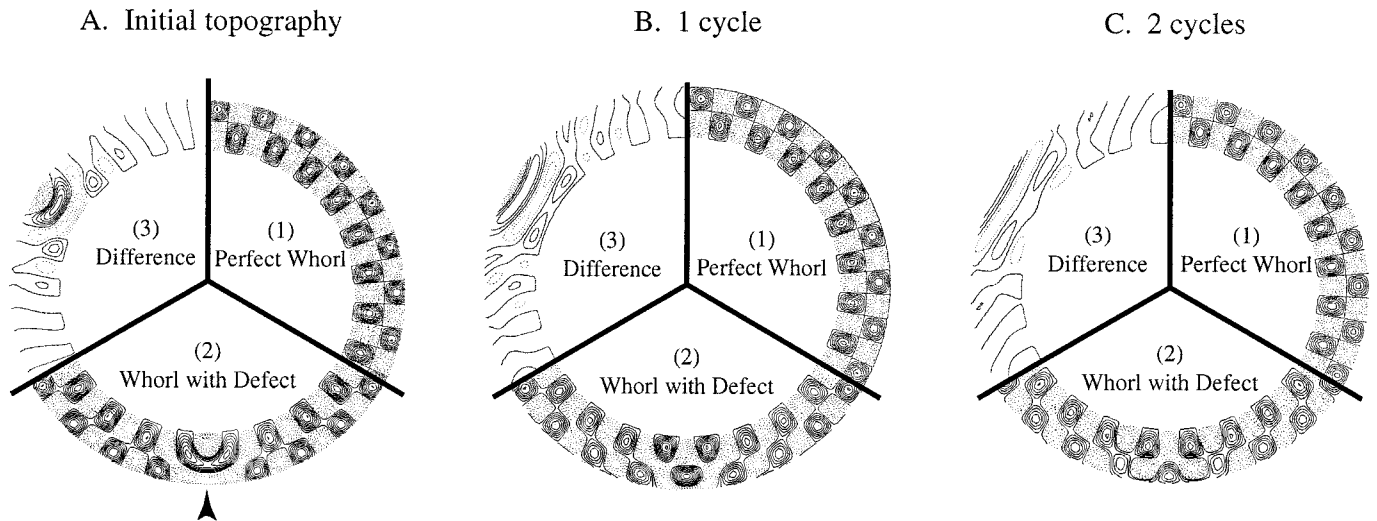


Fig. 6. Phyllotactic activity treated as cyclic and self-correcting buckling of topography on a formative annulus. Primordia are shown as humps (solid contour lines) alternating with depressions (dotted lines), which become creases. Propagation of whorls on an annulus with moving boundaries (propagation on a treadmill). This is the standard condition for vegetative growth but is rarely modeled. The whorled pattern is “checkerboard.” There is continuous patterning influence coming inward, continuous displacement outward. During the sequence shown, the material of the annulus is displaced outward by more than the annulus width by three stages over time. (A) (1) Regular whorl of nested undulations. (2) At bottom, the pattern has been intentionally disturbed. One peripheral primordium has been removed (arrowhead). (3) The topography of the perturbation is shown by the difference in topography between (1) and (2). In (B) and (C), note that the “error,” its difference from normal, diminishes as the “treadmill” operates. This appears to be the first explicit quantitative simulation, as topography, of self-correcting vegetative propagation. Simulation by Mr. Jonathan Fay and Dr. Arif Karabeyoglu (both at the Department of Aeronautics and Astronautics, Stanford University).

fixed. Now, however, physics in the horizontal plane becomes important. To implement buckling in three-dimensions, a torus was given a value for flexural rigidity and an elastic constant for the foundation. In the plant, only the upper half of the structure would be present. It represents an “incipient” whorl. By setting one mechanical property and varying the other by a factor of 2–4, it was possible to cause the confined torus to undulate either in the vertical plane, as with stamens, or in the horizontal plane, as with carpels (Fig. 7C, D). This led to a change in initial organ shape (humps vs. “cups”). Thus a prominent shape alternative can be accounted for by changing the value of a single material property.

An action of *DEFICIENS*, presumably affecting the plane of buckling, would be a very early aspect of expression of this gene, occurring before visible undulation. To act as structural “switches,” homeotic genes may show unusual pleiotropy in that they affect early organ-specific biophysical phenomena as well as later biochemical ones. That these two processes are separable has been shown by striking floral reversion studies (Battey and Lyndon, 1990).

CELL PATTERNING: ALIGNMENT FIELDS

The sections above, dealing with topography, envisioned two categories of input from the genome: one for a differential equation, the other for boundary conditions. I now apply this perspective to four small-scale structural features within a single undulation (primordium): organ axis, cell files, cellulose reinforcement, and microtubular cytoskeleton. These are normally coordinated in that files and growth direction run parallel to the organ axis and reinforcement is normal to it. This coherent association is not universal. Cell patterns can be random. Or, as in

ferns with single apical cells, cell division patterns can be complex but predictable. Thus, for cell pattern and presumably also cytoskeleton there is an apparent hierarchy of alternatives: unorganized vs. organized, with the latter subdivided into unidirectional and complex patterns.

The aim of this section is to see whether these “variations on a histological theme” reflect an optimization scheme parallel to that suggested for the larger scale phenomena of pattern and organ shape. No quantitative calculus-based theories have apparently been developed for this level. The proposal here is that a qualitative cytoskeletal tendency can substitute. This tendency may manifest itself as diverse stable secondary optimal configurations under various situations of organ shape and cell geometry. This is proposed to account for numerous cellular configurations seen in meristems that otherwise appear arcane.

Theory: a general tendency—The alignment of three features, i.e., cell files, cell growth direction, and cellulose microfibrils, can be reduced to cytoskeletal behavior (Green and Selker, 1991). The alignment of microtubules in cuboidal cells leads to a “hoop” reinforcement by cellulose. In meristems a cell typically has one characteristic alignment, although individual cell faces may differ quantitatively. This is most evident for cellulose reinforcement in the surface plane, which can be seen with polarized light (Green and Lang, 1981; Jesuthasan and Green, 1989). The correlation between reinforcement direction and microtubule alignment within a cell is relatively well established (Lang, Eisinger, and Green, 1982; Selker and Green, 1984; Sakaguchi, Hogetsu, and Hara, 1988). Active meristematic cells appear to have a general

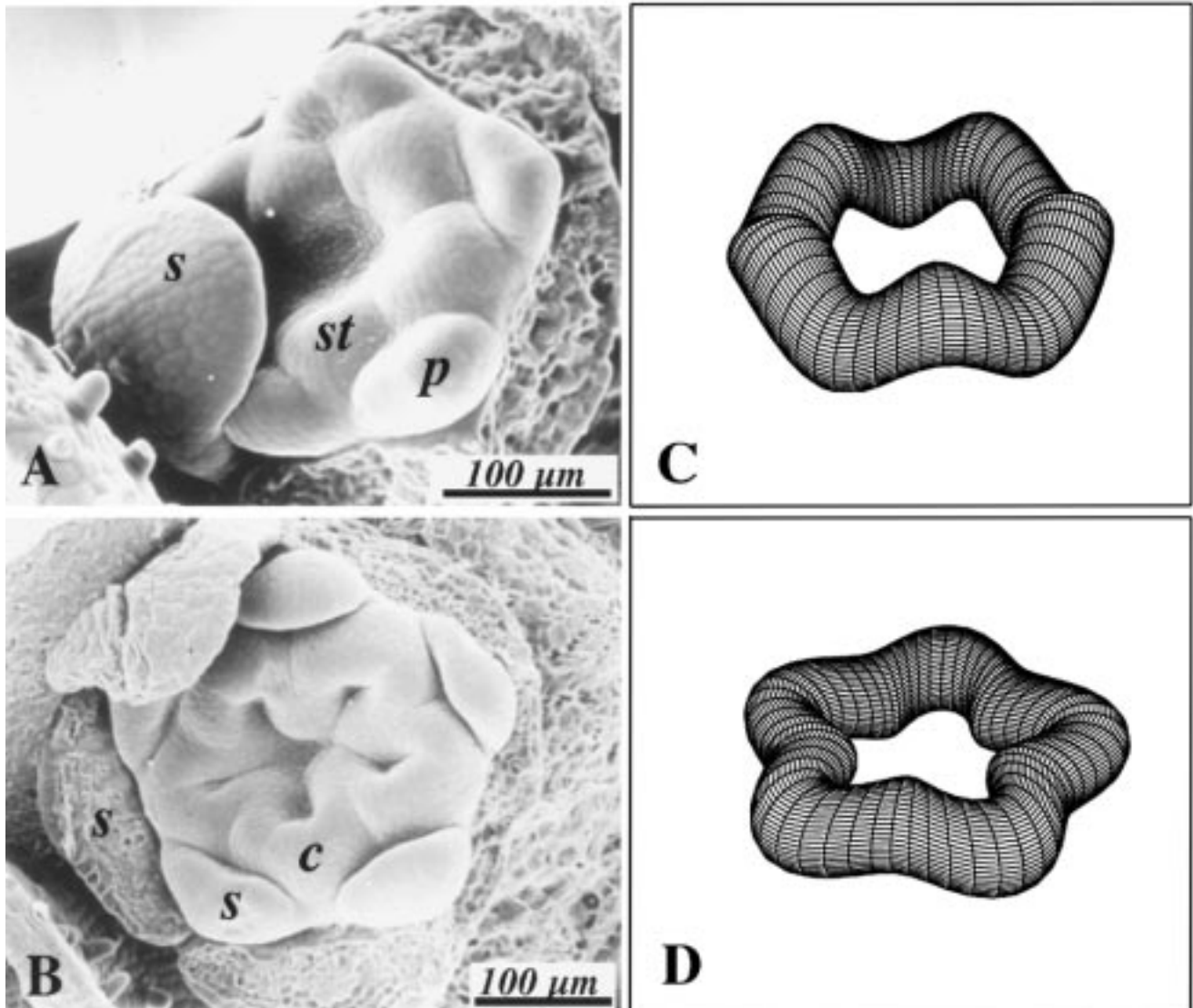


Fig. 7. Buckling and organ shape. (A) Wild-type stamens (*st*) in snapdragon arising in the third whorl. Creases traverse the formative zone, making a ring of humps. (B) The *deficiens* mutant of snapdragon where the first and second whorls are composed of sepals (*s*) and the third whorl is made of carpels (*c*). The formative region of the third whorl undulates in a plane as a ribbon, forming five cup-like primordia. (C, D) A preliminary continuum mechanical simulation. A ring is confined inside a fixed circular region. When heated or “forced to grow,” the excess length can be manifested as an out-of-plane undulation of five wavelengths. This simulates the normal development of stamens (as in A). When the ring develops in-plane undulation, the similarity is with carpels, showing the start of their cup-like structure (as in B). The orientation of the undulations in the model depends on the ratio of elasticity of the interior cells (corpus) and flexural rigidity of the epithelium (tunica). A change by a factor of 2 to 4 in one buckling parameter suffices to shift the plane of undulation. This mimics the change in the plane of undulation brought about by the *deficiens* mutation. This appears to be the first pertinent simulation. It is example 8 in Fig. 9. The derivation was done by Dr. Charles Steele (Department of Mechanical Engineering, Stanford University) from whom details can be obtained.

“hoop” arrangement for microtubules, covering four of the six faces. More developed cells, particularly epidermal cells, may have different alignments on different faces. The focus here is on the coherent hoop arrangement.

Alignment is reversibly sensitive to antimicrotubular drugs (Wasteneys and Williamson, 1989). Primary wall extension is normal to the reinforcement. Assuming that the division plane is typically inserted at right angles to the cytoskeletal alignment and the growth direction, as it is in proliferative divisions, aligned cytoskeletons generate a cell file.

There are many reports of small-scale features span-

ning the walls of cell groups. The best known is for xylem bar thickenings in adjacent tracheids (Sinnott and Block, 1945). Here the patterns clearly transcend cell boundaries. This cooperativity among cells is supported by observations that microtubules locally cluster on opposite sides of the new wall where these thickenings form (Hepler et al., 1993). Moreover, the parallel hoop-like microtubular arrays in adjacent cells in meristems commonly co-align (Sakaguchi, Hogetsu, and Hara, 1988).

If the intracellular microtubule alignment is combined with the intercellular tendency, a tissue-level tendency emerges: cuboidal cells tend to co-align their cytoskele-

tons in one direction. The production of parallel cell files and unidirectional growth follows. Such a coherent aggregate is called a reinforcement field (Green, 1994). If the co-alignment extends continuously around the organ axis, as a collar, the reinforcement situation is viewed as a primary available optimum. (The true optimum would be perfect parallel alignment on a flat plane.) In accord with the earlier paradigm, optimality is correlated with continuity and uniformity. Individual microtubules, and arrays of them, constantly “turn over.” Quantification of microtubule dynamics in living plant cells using fluorescence redistribution after photobleaching (FRAP) suggests that they perhaps maintain transverse alignment by an active self-cinching scheme (Hush et al., 1994). Thus, the proposal is for a dynamic, metabolism-dependent, mechanism for organizing cytoskeletal pattern among groups of cells. The suggested paradigm is that this alignment tendency will be sensitive to curvature and, when optimized, can explain many observed patterns (and the transitions among them).

Application—Configurations observed on apical domes—Because the apical dome usually has a significant curvature, a complete parallel reinforcement field is rarely seen. In some cases the cell and reinforcement pattern show no overall regularity. Clear examples are the surface of the apical dome of flowering *Anagallis* and *Vinca* (Hernández et al., 1991; Williams, 1991) and the central region of the sunflower capitulum. Here, presumably, the co-alignment tendency is not effective.

On the other hand, many meristems have a distinct cellular organization. There are two major types of organized cell patterns: those with a prominent noncuboidal cell (common in ferns) and those with many cuboidal cells (common in higher plants). In the fern *Onoclea*, the leaf apex has a single apical cell that is two-sided in surface view (Bierhorst, 1971). It is shaped like an orange segment and is not cuboidal. There is no directional reinforcement seen in the surface wall of the cell, but its quadrilateral derivatives have strong cellulose alignment (Lintilhac and Green, 1976). The tissue-level reinforcement pattern is suboptimal for two reasons: (a) there is the presence of the nondirectionally reinforced apical cell and (b) the aligned regions are disjointed. The two reinforcement fields, produced sequentially from alternate sides of the apical cell, abut each other at 90° (Fig. 8A, 1). Thus the reinforcement pattern below the apical cell is a mosaic of two fields. The line of juxtaposition shows sharp angular discontinuity of cellulose alignment, striking in polarized light (Fig. 8A, 2). In the shoot apex of the same plant, the apical cell is three-sided. There are three reinforcement fields (Fig. 8A, 3). It is perhaps noteworthy that noncuboidal cells often divide for several cycles. Repeated division is known for some three-sided cells that produce groups of cells that make stomata (Sylvester, Smith, and Freeling, 1996).

In higher plants, the apical dome has long been known to have fields of surface cells, parallel files, distinguishable histologically (Lyndon, 1998). These tend to run between the base of a recent leaf and the tip of the dome. Investigation with polarized light shows that these groups of cells are single reinforcement fields (Green, 1986, 1994). They are in distinctive patterns. In the alternate-

leafed (distichous) *Tradescantia* and the opposite-leafed (decussate) *Vinca* there are three fields (Jesuthasan and Green, 1989; Fig. 8B). The apex is typically elliptical. A long central corridor, with transverse reinforcement across it, runs down the long axis. On either side, near the summit, are flanking lenticular-shaped fields with alignment at 90° to that of the corridor. Thus 90° angular contrast is present, as with *Onoclea*. However, at the margin of the dome the alignments blend together to make a single field (Fig. 8B).

In plants with alternating whorls of three leaves, the corresponding three-fold symmetrical arrangement is seen (Green, 1986). In plants with spiral phyllotaxis, e.g., *Ribes*, an equivalent asymmetrical arrangement is observed. Thus, well-defined mosaics of surface reinforcement fields are found widely among ferns and higher plants. In all cases, they comprise discontinuous approximations of the optimal available configuration: a single transversely oriented field encircling the axis. The axis is indeed encircled, but in partly disjointed fashion. There is a systematic character to the transitions between these various configurations.

Transitions between configurations—The simplest is seen on apical domes. As noted, in higher plants the disjointed mosaic of fields near the tip of the dome intergrades into a single optimal field at the base, or periphery, of the dome. However, in *Onoclea* signs of discontinuity of alignment persist (Fig. 8A). Perhaps cell-to-cell communication, promoting co-alignment, is slow across lines where the cells are of different age.

In the decussate plant *Vinca*, the alignment in the corridor region of the dome is transverse to the long axis of the corridor. Since the long axis of the ellipse changes by 90° during each plastochron, the alignment of the cells at the tip of the dome also changes. The new central alignment after the change is parallel to that at the base of the new-forming leaves, thus bridging the two former flanking alignments. The alternating orientation here is statistically canceling. As with the single apical cell of *Onoclea*, there is no net alignment. There is a third way of having indeterminacy at the very pole. In tricussate apices with three “corridors,” a 90° alternation cannot be compatible with the three corridors. An unorganized pattern is seen where such corridors converge (Green, 1986; Fig. 8B).

A different type of transition occurs when a part of a single reinforcement field develops into a new axis (Fig. 8C). In vegetative phyllotaxis, this occurs at the periphery of reorganizing apical domes where they initiate primordia. As studied in *Graptopetalum* with polarized light for cellulose, and with electron microscopy for microtubules, the alignment revision involves two steps (Hardham, Lang, and Green, 1980; Green and Lang, 1981; Selker and Green, 1984). In association with bulging, there is a 90° discontinuity, a sharp shift in alignment, in a central band-like region. The cell shifts have been individually described in *Vinca* (Jesuthasan and Green, 1989) and *Graptopetalum* (Green, 1984). Such shifted regions make a new “corridor” in a mosaic because there is now a central stripe of one alignment, with two lateral regions of opposing alignment. Note that, as with ferns, this three-field arrangement is a rough approximation of

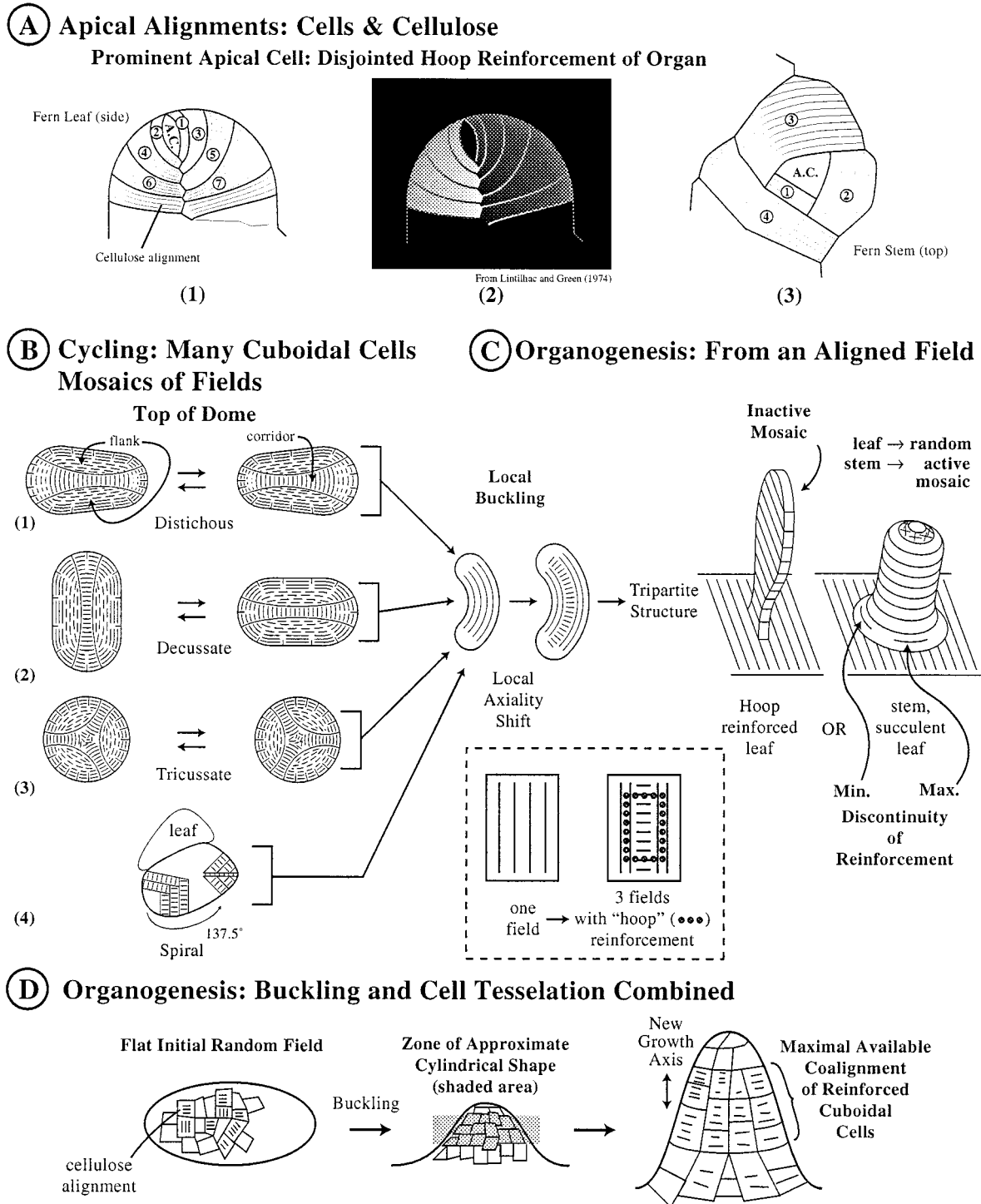


Fig. 8. Observations suggesting a tessellation-optimization paradigm for expression of cell and reinforcement pattern. (A) A system with a prominent nondirectionally reinforced apical cell. *Onoclea*. (1) The segmentation pattern produces a left-right alternation of curved cuboidal cells, each directionally reinforced (thin lines). The directions oppose at 90° in a zig-zag line at center. (2) The apex in polarized light, compensator present (from Lintilhac and Green, 1976). The brightness/darkness shows 90° confrontation of alignments. (3) Corresponding alignments in the three-sided apical cell of the shoot. Note approximation of overall hoop reinforcement of the organ tip. (B) Top view of higher plant apical domes. Fine lines show cellulose alignment as seen in polarized light. Cells are not shown, but cell axes are normal to cellulose alignment (1–4). Four types of cycling reinforcement fields (after Green, 1986). Cyclic transitions during the plastochron are shown by double arrows. Each mosaic has one or more central corridor bands, flanked by lentoid regions. Near, and sometimes also at, the center of the dome, there is sharp alignment contrast between corridors and the regions flanking them. This contrast is not present at the periphery. There the alignments become blended, particularly at the base of the curved dome, which is more cylindrical. (C) New organ formation from an aligned field. Here a 90° reorientation occurs at the periphery of the dome to generate three fields from one. The new alignments provide four directions of reinforcement for the initial, approximate, hoop reinforcement of the new organ (see box). The unused remnants of a single original field are clearly seen in Fig. 3G. The process can produce new leaves or shoots. (D) New organ formation from a random field. Here, during division, quadrilateral cells progressively optimize co-alignment in the midregion of the new hump where the shape best approximates a cylinder. This shape both localizes and sets the new reinforcement direction. This produces a primary optimal alignment field. This relationship couples the processes at the small scale (curvature-sensitive tessellation by reinforced cuboidal cells) with buckling, the larger scale processes, which produces curvature. This provides geometrical/angular coherence across scales.

a large-scale “hoop” reinforcement pattern (Fig. 8C). It is approximate because the center has alignment and because the reinforcement lines are rectangular, rather than circular. As on the established dome, these discontinuities smooth out as the tissue develops (moves relatively downward onto a more cylindrical region). A record of this geometrical revision, involving a 90° shift, is clearly seen in an image of a new stem in *Graptopetalum* where remnants of the original single field are prominent (Fig. 3G).

This sequence has been established in great detail for leaf and stem formation in *Graptopetalum* (Tiwari and Green, 1991). It appears to occur first for the leaf. Cell organization soon becomes random at the leaf tip. In this system leaf initiation can occur in isolation (Green and Brooks, 1978). In such cases the forming leaf appears to “induce” the surrounding cells to form a miniature stem under the single leaf (Green, 1984). It thus appears that in *Graptopetalum* there are four stages to stem production: ridge formation, reinforcement shifts (to generate hoop reinforcement), leaf formation, and stem formation. The last appears to be induced by the aggregate of leaves formed previously.

Using polarized light, a remarkably similar sequence was seen for leaf initiation in the distantly related aquatic plant *Hippuris*, formerly *Anacharis* (Green, 1986). Both *Graptopetalum* and *Hippuris* produce a three-part orientation mosaic despite the fact that the geometry of the formative regions is different. In *Graptopetalum* the leaves form de novo atop an elongate ridge. In *Hippuris* they form in sequence on the flanks of a nearly cylindrical apex.

Observing cell division and growth orientation, a 90° shift in cells in a band-like region was also seen during leaf formation on explanted axillary stem tissue of watercress, *Nasturtium officinale* (Selker and Lyndon, 1996). The cell pattern was the same as for leaf formation in *Graptopetalum* and *Hippuris*, forming a three-part orientation mosaic.

The basis for the 90° shift in cellulose orientation, presumably the critical initiating discontinuity, is not known. Such shifts correlate with the long axis of newly formed daughter cells and with the orientation of the recent cross wall between the cells (Green, 1984). For organogenesis, the key shift may be brought on by a cytoskeletal response to directional stretch on a curved surface, a feature of buckling.

The final case of field initiation is the simple one where a part of a large unorganized field develops into a single field (Fig. 8D). This is observed histologically, for example, on the capitulum of sunflower when new organs form or on the floral primordium of *Anagallis* when sepals arise (Hernández et al., 1991). New longitudinal files simply appear midway up the primordium as it bulges out. They are not present beforehand.

A qualitative optimization model based on cytoskeletal behavior—The diverse configurations above are proposed to be alignment states, which are either at the primary available optimum (a single collar-like field) or are at secondary optima (disjointed approximations). The states are interconvertible. A qualitative algorithm based on the maximally coherent tessellation, or uniform

tiling, of a surface with quadrilateral units appears capable of reproducing much of the phenomenology. The model predicts cell pattern on the basis of the inferred relative stability of cytoskeletal alignments of adjacent cells. It is a preliminary attempt at explaining cell pattern and reinforcement, based on limited data. The key observations and key assumptions are summarized below.

a) Meristematic cuboidal cells have hoop-like cytoskeletal arrays. The alignment is often particularly prominent on the external periclinal face. Here cellulose birefringence is strong and the physical forces for elongation are concentrated.

b) Noncuboidal cells have no prominent internal alignment. Such cells can divide and often do so in regular segmentation patterns. Their quadrilateral derivatives do have alignment.

c) Microtubular arrays in adjacent cuboidal cells tend to co-align. Mutual adjustments, toward improving co-alignment, occur at cell division.

d) A hierarchy of stability among the possible cell to cell interfaces is postulated.

1) Parallel transverse alignment is most stable.

2) Perpendicular alignment is second.

3) Aligned to random is third.

4) Random to random is fourth.

e) Among aggregates of dividing cells, the maximum stability possible is realized (by trial and error through the flexibility at cell division).

f) Maximum stability is a function of curvature. The available optimum configuration is co-alignment on a cylindrical surface where there is curvature only in one direction. The other configurations are secondary optima largely because uniform tessellation by rectangles is not possible on a dome surface, especially near the pole. Thus in a three-dimensional sinusoidal undulation, co-alignment is maximal in the midregion and precluded at the pole. *This couples buckling phenomena at the topographical level to phenomena at the cellular level.*

Two assumptions are needed to explain further coordination during organogenesis in vegetative and floral apices (Green, 1994):

g) Cells at the organ pole become nonmeristematic and produce a downwardly mobile activator of co-alignment. This can explain why, in vegetative systems, leaf tips are inactive morphogenetically, while the proximal part of the leaf and the apical dome tend to show strong co-alignment.

h) In flowering, co-alignment appears to be missing on smooth large domes. Perhaps some key factor is not produced (i.e., bracts may not make it). Curved distal regions of new primordia, with factor, would account for the new co-alignment arising below the tip.

Although the list of assumptions is long, they are plausible. The proposed hierarchy simply reflects the relative frequency of interfaces seen in the various situations. So the paradigm has passed only the test of relative efficiency. Note that there are two important “uphill” or non-spontaneous transitions: (a) formation of single fields from an unorganized array and (b) the formation of a three-part mosaic from a single field. Both appear associated with a local buckling process. The other transitions are spontaneous or “downhill” in that overall co-alignment is simply improved by reduction of curvature. To-

gether, cycles of transitions can occur. Note that the anisotropy of reinforcement can influence the buckling process (influencing initial shape) so interaction between levels, in both directions, is plausible. On this important point Williamson (1991) has presented a critique, and a model, for the interplay between wall stretching and microtubule behavior.

These rules offer a framework to attempt to explain the histological sequences following physical perturbation as mentioned above: organ induction by expansin, by large-scale constraint on sunflower, and by local mechanical constraint on *Graptopetalum* which produced an ectopic row of histologically normal leaves (Fig. 3). This cytoskeletal scheme, combined with the buckling activity, has the potential to reduce a very wide range of phenomena to only two issues for a plane of cells: (a) what causes it to fold in a particular way and (b) how does that folding interact with cytoskeletal phenomena? These both respond to previous folding and influence future folding, completing a stable set of two-way biophysical interactions.

Some previous theory on this subject has concerned encoding the sequence of divisions (Korn, 1993). Other theory accounts for the striking orthogonal histological patterns in roots in terms of tensors (Hejnowicz and Karczewski, 1993). The latter work shares with this treatment the emphasis on orthogonality and the fundamental feature that observed patterns reflect alternative self-stable activities, governed by boundary conditions. The present model adds the variable of reinforcement direction by cellulose, the involvement of the cytoskeleton, as well as an application to the broader array of surface cell patterns seen in shoots and flowers.

DISCUSSION

An apparent salient feature of the geometry of plants is the propagation of, and the transition between, a limited number of distinctive patterns. These can be regulated by the genome in a two-category format of expression, as broadly interpreted here. One category takes the form of parameters for an activity expressed as a differential equation. That is, conventional products of gene activity such as cellulose synthesis and microtubule polymerization have their influence on geometry only after being converted to biophysical parameters (e.g., bending stiffness) or dynamic activity (microtubule alignment). This can be paraphrased as a latent tendency. For organ patterning and shape, a tissue tends to buckle at a standard intrinsic wavelength. For alignment features within a primordium, the microtubular cytoskeletons, considered

to be like hoops around a barrel, tend to co-align laterally to give the key tendency.

The second category is the geometry of the system as specified by boundary conditions. For example, annulus width is critical for organ pattern and curvature influences the "annealing" of microtubules. The schemes at the topographical and cellular levels are physically coupled to provide coherence of geometry from cytoskeletal features to organ pattern. It goes without saying that the genome also provides other essentials such as turgor pressure, synthesis for growth, etc.

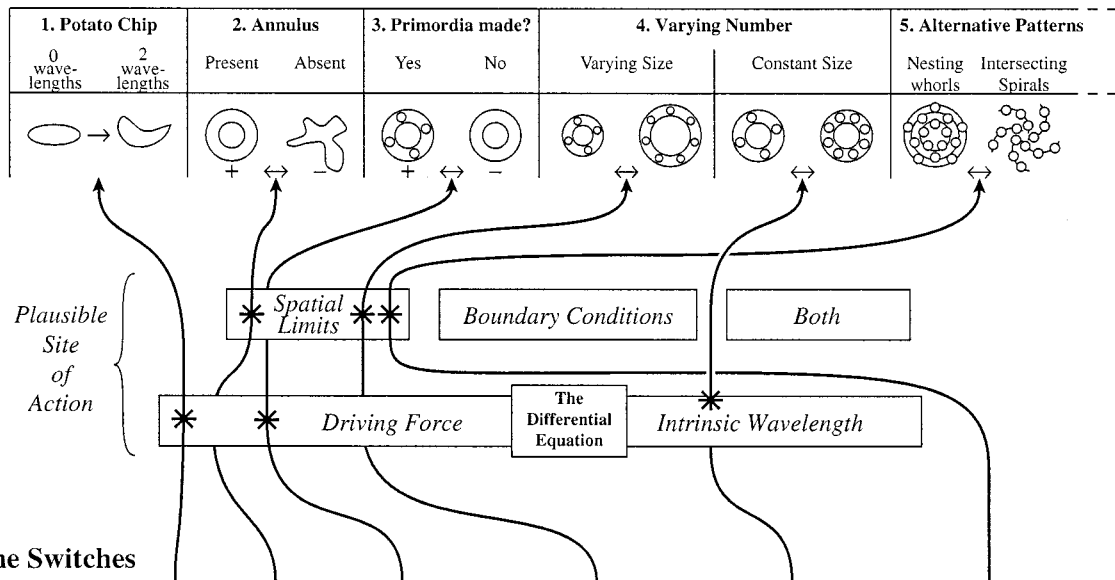
The potential broad applicability of this perspective for organ pattern is given by examples in Fig. 9. It is a speculative interpretation of well-known structural change phenomena in terms of the buckling paradigm. It presents, at the top, an array of structural pairs that are either alternative manifestations of a developmental process (mutant vs. wild type) or unusual one-time conversions of structure. For each case, a connection is made to an apparent pertinent genetic change, or experimental treatment, regarded as the potential cause for the particular transition. These are shown at the bottom. In between, in boxes, lie the two categories of causal input (Fig. 1B) of the current paradigm in expanded form. A plausible localized site(s) of action, within the paradigm, for each switch is shown by an asterisk.

On positional information—The differential-integral format presents cause and effect in a different way than that employed in positional information theory. A main feature of positional information is that the nature of the signal and that of the response are independent. This gives the format extreme flexibility. In the present case there are two main differences. First, in buckling flexibility is limited, i.e., there are only a limited number of optima. This developmental constraint can explain D'Arcy Thompson's comment about phyllotaxis "... not the least curious feature ... is the small number of possible arrangements which we observe and recognize" (Thompson, 1942). Second, the signal and its interpretation are virtually the same process. With a latent intrinsic wavelength present, there can be a localized response without a local signal. The signal, in-plane stress, is not localized or patterned within the formative area. As an everyday example, there is no saddle-shaped input to produce a saddle-shaped potato chip, a product of buckling of a flat disk. The structure thus develops internal periodicity solely because this is the minimum energy solution for the system as a whole. This view is well known in animal work through the models of Steinberg (Steinberg and Poole, 1981) and Odell and co-workers (Odell

→

Fig. 9. Speculative application of the paradigm to diverse structural alternatives, many of which are covered in the text. The structural alternatives may be differences between wild-type and mutant or unusual one-way transitions. The switches may be mutation, chemical, or physical treatment. Ten structural alternatives (above) are connected to ten apparent controlling "switches" (below) via a differential-integral transduction (boxes in between). Each switch is connected to the structural alternatives by a line. On each line, the component of the differential equation, or of the boundary conditions, whose variation correlates with change in structure is shown by an asterisk. Note that combinatorial and pleiotropic effects exist with this type of transduction. Most of the examples are well known. This includes, as number 1, potato chip formation, which by buckling provides two wavelengths of topography, *de novo*. Numbers 2 and 3 are common mutants. Others are covered in the text. These include varying numbers per whorl (number 4) and the spiral-whorl transition (number 5). Number 6 reflects the work of Green and co-workers (Green, Steele, and Rennich, 1996). In example number 7, snapdragon, the fifth stamen is often vestigial. From images of the topography (supplied by Dr. Hans Sommer, Max Planck Institute, Köln) it appears that adjacent whorls locally superimpose. Because they are out of phase there, destructive interference

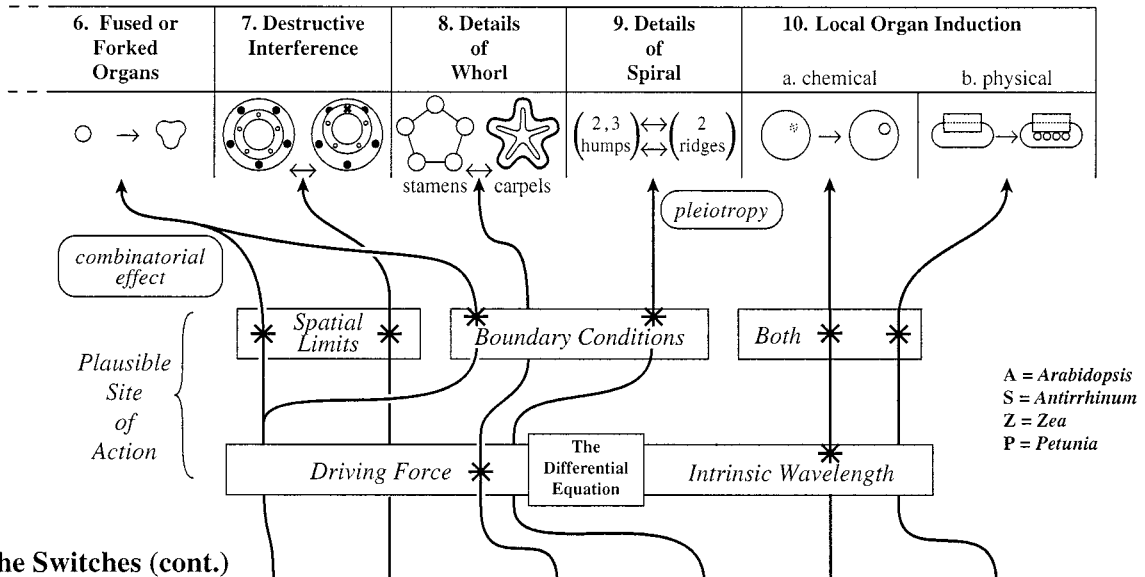
I. The Structural Alternatives



II. The Switches

Mutation:		<i>raspberry</i> (A)	<i>pin</i> (A) <i>concentric</i> (P)	<i>abphyl</i> (Z) <i>cadastral genes</i> (A) <i>pallida</i> (S)	<i>cycloidea-680</i> (S) <i>ettin</i> (A) <i>perianthia</i> (A)	<i>leafy</i> (A)
Treatment:	<i>cook</i>				<i>cytokinin application</i>	<i>GA on ivy</i>

The Structural Alternatives (continued)



The Switches (cont.)

Mutation	<i>leafy</i> (A)	<i>cycloidea</i> (S)	<i>deficiens</i> (S)	<i>floricaula</i> (S)		
Treatment					<i>Expansin</i> (chemical)	<i>Glass chip</i> (physical)

would be expected in the region of overlap, perhaps leading to reduced development. Number 8 is the organ shape alternative (carpels/stamens). Of special interest is the pleiotropic effect of *floricaula* (number 9) in the inflorescence of snapdragon where the higher number of spirals is dropped and humps convert to ridges. This transition appeared on the cover of *The Plant Cell* in December 1995. In continuum mechanics this pair of effects can reflect the wavelength of the patterning influence being too short for the wavelength of the formative annulus. The examples in number 10, chemical or physical induction of organ and organ pattern, are covered in the text. It is seen that many "switches" can be connected to a wide range of structural alternatives by single changes in intermediate components of a differential-integral relation. This widespread covariation is the main justification for presentation of the paradigm.

et al., 1981). It has the unusual aspect that large-scale features (boundary conditions specified over a large area) determine events at a smaller scale.

Another special feature, involving differential equations, is that the constant features of the equation best re-encapsulate the basis of the mechanism. Because of the mathematical complexity, the unknown equation is hard to deduce from the usual tactic of correlating variation in input with variations in output (Green, 1996). That is, in studying diverse responses to perturbation, e.g., mutation, it is the part of the system that does not change in concert with variation of response that is revealing (and elusive). Thus, for spiral vs. whorled phyllotaxis, the buckling equations are the same. It is how the same system responds differently to different boundary conditions that is the apparent key to understanding.

On evolution—The perspective here is that natural selection acts on the alternative stable developmental activities as seen in the wild type. These can be interchanged by major perturbations either during evolution or development. When nondiscrete alternatives appear (e.g., disorganized or hybrid organs), the components for stability, such as those proposed here, are missing. Selection thus appears to act on a set of related functional alternatives which can be readily interconverted in the short run (development) or the long run (evolution). These features are readily encompassed in the differential-integral format.

With regard to D'Arcy Thompson's comment on pattern number seen in nature, these few regular patterns are few, presumably because they are stable (optimized) structures, capable of cycling. This is likely to be a small set. For Darwin, the observed patterns appear nonintuitive or maddening because their common basis is seen only with the proper mathematical paradigm.

On the organism-cell distinction—Extensive discussion has centered on the issue of the prevalence of cellular vs. organismal factors in higher plant development (Kaplan and Hagemann, 1991; Cooke and Lu, 1992). The present paradigm puts emphasis on certain continuum mechanical phenomena, which, while at the tissue level, do not require cells per se. These phenomena generate topography and thereby connect tissue to organ shape and organ arrangement. On the other hand, the production of organ-level hoop-reinforcement for the growth direction appears to be fully dependent on the cytoskeletal behavior of individual cells. The arcane geometry of the *Onoclea* leaf apex (Fig. 8) appears to reflect a striking compromise between the "need" for hoop reinforcement at the organ level and the restriction that it be generated on a cell-by-cell basis. The two contrasting perspectives become complementary.

On combinatorial and pleiotropic responses—It is not widely recognized that the phenomena of combinatorial and pleiotropic interactions exist not just at the molecular level, but also within the differential-integral format in the solid state. A quantitative change in a single boundary parameter for buckling can lead to two concurrent changes in manifestation. For example, in aberrant spiral phyllotaxis (*floricaula*) (Carpenter et al., 1995; Fig. 9) there

are two consequences. One set of spirals and the hump-like character of primordia are lost together. This is pleiotropy. On the other hand, to obtain fused primordia by buckling, a change in both the width of the formative area and its boundary conditions (hinged vs. clamped) can be necessary (Green, Steele, and Rennich, 1996). This is combinatorial action. It is clear that similar phenomenology can have a macroscopic as well as a molecular basis.

There is no doubt that the genome specifies an astronomical number of events that occur predictably in both time and space. In morphogenesis, the final manifestation is geometrical and physical: a shape, a pattern, an alignment. Most current suggestions for the specification emphasize the role of myriad interactions that are (a) at the molecular level and (b) are reducible to issues of promotion and inhibition. This is often thought to scale up, with many interactions, to account for details at higher levels of organization. This article suggests that much of such activity is a prelude to other transductions that can be understood only by involving the supermolecular level of organization explicitly. The tactic here has been to start with phenomena at the epithelial level. One can then scale up to patterning and organ form and down to cell pattern and reinforcement direction. Because the transductions that bring on change take the form of differential-to-integral, the pertinent gene products need to be converted to biophysical parameters. The boundary conditions at both structural levels (curvature in two and three dimensions) overlap, allowing for coordination between levels.

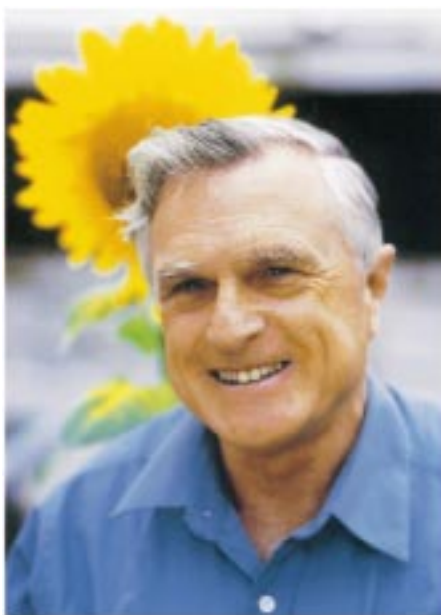
Thus by adding calculus and biophysics, the features of stability, coherence, and geometrical specificity can be added explicitly to the well-known essential genetic controls pertinent to patterning and morphogenesis. This article has pointed out that the added context has three salient features. (a) The pertinent analytical part of the context, e.g., the set of latent tendencies can be as challenging and essential to understanding as the nature of the molecular control itself. The tangible part of the context, the parameters for the pertinent equation and boundary conditions, are products of the genome. (b) The switch, effective in the particular context, is usually a change in the boundary conditions. In some cases, parameters or values in the equation itself may change to act as a switch (e.g., to change wavelength). In either event, these parameters are likely to be "far downstream," i.e., considerably derived from products of conventional expression sought in screens. (c) An unknown context is difficult to seek. A common tactic, used here, is to consider what is **sufficient** to account for the demonstrable complexity of the normal process itself. In this case, for patterning the buckling analogy was explored. For explaining mechanisms where calculus is heavily involved, this tactic appears to be necessary. It is added to, and contrasts with, the extensive information derived from the perturb-and-assay interventions (against constant background), which deal with what is **essential** to cause the developmental outcome to change (see Green, 1996). Adding the gene-produced biophysical context to the well-known promotion-inhibition phenomenology broadens the view of genetic control of a process

to provide a more general grasp, approximating genetic basis.

LITERATURE CITED

- BATTEY, N. H., AND R. F. LYNDON. 1990. Reversion of flowering. *Botanical Review* 56: 162–189.
- BERDING, C., T. HARBICH, AND H. HAKEN. 1983. A pre-pattern formation mechanism for the spiral-type patterns of the sunflower head. *Journal of Theoretical Biology* 104: 53–70.
- BERNASCONI, G. P. 1994. Reaction-diffusion model of phyllotaxis. *Physica D* 70: 90–99.
- BIERHORST, D. W. 1971. Morphology of vascular plants. Macmillan, New York, NY.
- CARPENTER, R., L. COPSEY, C. VINCENT, S. DOYLE, R. MAGRATH, AND E. COEN. 1995. Control of flower development and phyllotaxy by meristem identity genes in *Antirrhinum*. *Plant Cell* 7: 2001–2011.
- CHAPMAN, J. M., AND R. PERRY. 1987. A diffusion model of phyllotaxis. *Annals of Botany* 60: 377–389.
- COOKE, T. J., AND B. LU. 1992. The independence of cell shape and overall form in multicellular algae and land plants: cells do not act as building blocks for constructing plant organs. *International Journal of Plant Sciences* 153: S7–S27.
- DARWIN, F. [ED.] 1897. The life and letters of Charles Darwin: including an autobiographical chapter. Appleton, New York, NY.
- ERICKSON, R. O. 1983. The geometry of phyllotaxis. In J. E. Dale and F. L. Milthorpe [eds.], *The growth and functioning of leaves*, 53–88. Cambridge University Press, Cambridge.
- FLEMING, A. J., S. MCQUEEN-MASON, T. MANDEL, AND C. KUHLEMEIER. 1997. Induction of leaf primordia by the cell wall protein expansin. *Science* 276: 1415–1418.
- FUJITA, T. 1939. Statistische Untersuchungen über den Divergenz-winkel bei den schraubigen Organstellungen. *Botanical Magazine, Tokyo* 53: 194–199.
- GIDDINGS, T. H., AND L. A. STAEHELIN. 1991. Microtubule-mediated control of microfibril deposition: a re-examination of the hypothesis. In C. W. Lloyd [ed.], *The cytoskeletal basis of plant growth and form*, 85–99. Academic Press, New York, NY.
- GREEN, P. B. 1984. Shifts in plant cell axiality: histogenetic influences on cellulose orientation in the succulent *Graptopetalum*. *Developmental Biology* 103: 18–27.
- . 1986. Plasticity in shoot development: a biophysical view. In D. H. Jennings and A. J. Trewavas [eds.], *Plasticity in plants*, 211–232. Cambridge University Press, Cambridge.
- . 1994. Connecting gene and hormone action to form, pattern, and organogenesis. *Journal of Experimental Biology* 45: 1775–1788.
- . 1996. Transductions to generate plant form and pattern: An essay on cause and effect. *Annals of Botany* 78: 269–281.
- , AND K. BROOKS. 1978. Stem formation from a succulent leaf: its bearing on theories of axiation. *American Journal of Botany* 65: 13–26.
- , AND J. M. LANG. 1981. Toward a biophysical theory of organogenesis: birefringence observations on regenerating leaves in the succulent, *Graptopetalum paraguayense* E. Walther. *Planta* 151: 413–426.
- , AND J. M. L. SELKER. 1991. Mutual alignments of cell walls, cellulose, and cytoskeletons: their role in meristems. In C. W. Lloyd [ed.], *The cytoskeletal basis of plant growth and form*, 303–322. Academic Press, New York, NY.
- , C. S. STEELE, AND S. C. RENNICH. 1996. Phyllotactic patterns: a biophysical mechanism for their origin. *Annals of Botany* 77: 515–527.
- , AND ———. 1998. How plants produce pattern: a review and a proposal that undulating field behavior is the mechanism. In R. V. Jean and D. Barabé [eds.], *Symmetry in plants*, 359–392. World Scientific, Singapore.
- GUNNING, B. E. S., AND D. R. HARDHAM. 1982. Microtubules. *Annual Review of Plant Physiology* 33: 651–698.
- HARDHAM, D. R. 1982. Regulation of polarity in tissues and organs. In C. W. Lloyd [ed.], *The cytoskeleton in plant growth and development*, 377–403. Academic Press, London.
- , J. M. LANG AND P. B. GREEN. 1980. Reorganization of cortical microtubules and cellulose deposition during leaf formation in *Graptopetalum paraguayense*. *Planta* 149: 181–195.
- HARRISON, L. G. 1993. Kinetic theory of living pattern. Cambridge University Press, New York, NY.
- , AND N. A. HILLIER. 1985. Quantitative control of *Acetabularia* morphogenesis by extracellular calcium: a test of kinetic theory. *Journal of Theoretical Biology* 114: 177–192.
- , J. SNELL, J. VERDI, D. E. VOGT, G. D. ZEISS, AND B. R. GREEN. 1981. Hair morphogenesis in *Acetabularia mediterranea*: temperature-dependent spacing and models of morphogen waves. *Protoplasma* 106: 211–221.
- HEJNOWICZ, Z., AND J. KARCZEWSKI. 1993. Modelling of meristematic growth of root apices in a natural co-ordinate system. *American Journal of Botany* 80: 309–315.
- HEPLER, P. K., A. L. CLEARY, B. E. S. GUNNING, P. WADSWORTH, G. O. WASTENEYS, AND D. H. ZHANG. 1993. Cytoskeletal dynamics in living plant cells. *Cell Biology International* 17: 127–142.
- HERNÁNDEZ, L. F., AND P. B. GREEN. 1993. Transductions for the expression of structural pattern: analysis in sunflower. *Plant Cell* 5: 1725–1738.
- , A. HAVELANGE, G. BERNIER, AND P. B. GREEN. 1991. Growth behavior of single epidermal cells during flower formation: sequential scanning electron micrographs provide kinematic patterns for *Anagallis*. *Planta* 185: 139–147.
- HOLLOWAY, D. M., AND L. G. HARRISON. 1999. Algal morphogenesis: modelling interspecific variation in *Micrasterias* with reaction-diffusion patterned catalysis of cell surface growth. *Philosophical Transactions of the Royal Society of London* 354: 417–433.
- HUSH, J., P. WADSWORTH, D. A. CALLAHAM, AND P. K. HEPLER. 1994. Quantification of microtubule dynamics in living plant cells using fluorescence redistribution after photobleaching. *Journal of Cell Science* 107: 775–784.
- JEAN, R. V. 1994. Phyllotaxis. Cambridge University Press, New York, NY.
- JESUTHASAN, S., AND P. B. GREEN. 1989. On the mechanism of decussate phyllotaxis: biophysical studies on the tunica layer of *Vinca major*. *American Journal of Botany* 76: 1152–1166.
- KALTHOFF, K. 1996. Analysis of biological development. McGraw-Hill, New York, NY.
- KAPLAN, D. R., AND W. HAGEMANN. 1991. The relationship of cell and organism in vascular plants: are cells the building blocks of plant form? *BioScience* 41: 693–703.
- KORN, R. W. 1993. Apical cells as meristems. *Acta Biotheoretica* 41: 175–189.
- KWIATKOWSKA, D. 1995. Ontogenetic changes of phyllotaxis in *Anagallis arvensis* L. *Acta Societatis Botanicorum Poloniae* 64: 319–325.
- LACALLI, T. C. 1981. Dissipative structures and morphogenetic pattern in unicellular algae. *Philosophical Transactions of the Royal Society of London* B294: 547–588.
- LANG, J. M., W. R. EISINGER, AND P. B. GREEN. 1982. Effects of ethylene on the orientation of microtubules and cellulose microfibrils of pea epicotyl cells with polylamellate cell walls. *Protoplasma* 110: 5–14.
- LINTILHAC, P. M., AND P. B. GREEN. 1976. Patterns of microfibrillar order in a dormant fern apex. *American Journal of Botany* 63: 726–728.
- LLOYD, C. W., AND P. W. BARLOW. 1982. The co-ordination of cell division and elongation: the role of the cytoskeleton. In C. W. Lloyd [ed.], *The cytoskeleton in plant growth and development*, 203–228. Academic Press, London.
- LYNDON, R. F. 1994. Control of organogenesis at the shoot apex. *Tansley Review Number* 74. *New Phytologist* 128: 1–18.
- . 1998. The shoot apical meristem, its growth and development (Developmental and cell biology series). Cambridge University Press, Cambridge.
- MARC, J., AND W. P. HACKETT. 1991. Gibberellin-induced reorganization of spatial relationships of emerging leaf primordia at the shoot apical meristem in *Hedera helix* L. *Planta* 185: 171–178.
- MEICENHEIMER, R. D. 1981. Changes in *Epilobium* phyllotaxy induced by N-1-naphthylphthalamic acid and α -4-chlorophenoxyisobutyric acid. *American Journal of Botany* 68: 1139–1154.
- . 1998. Decussate to spiral transitions in phyllotaxis. In R. V.

- Jean and D. Barabé [eds.], Symmetry in plants, 125–143. World Scientific, Singapore.
- MEINHARDT, H. 1995. The algorithmic beauty of sea shells. Springer-Verlag, Berlin.
- MEYEROWITZ, E. M. 1996. Plant development: local control, global patterning. *Current Opinion in Genetics and Development* 6: 475–479.
- MINGO-CASTEL, A. M., C. GOMEZ-CAMPO, M. E. TORTOSA, AND A. M. PELACHO. 1984. Hormonal effects on phyllotaxis of *Euphorbia lathyris* L. *Botanical Magazine, Tokyo* 97: 171–178.
- MITCHISON, G. J. 1977. Phyllotaxis and the Fibonacci series. *Science* 196: 270–275.
- MURRAY, J. D. 1981. A pre-pattern formation mechanism for animal coat markings. *Journal of Theoretical Biology* 88: 161–199.
- ODELL, G. M., G. OSTER, P. ALBERCH, AND B. BURNSIDE. 1981. The mechanical basis of morphogenesis. I. Epithelial folding and invagination. *Developmental Biology* 85: 446–462.
- RASMUSSEN, N. 1991. Studies on the determination of organ pattern and organ identity in flower development. Ph.D. dissertation, Biological Sciences, Stanford University, Stanford, CA.
- RIDLEY, J. N. 1982. Packing efficiency in sunflower heads. *Mathematical Biosciences* 58: 129–139.
- SAKAGUCHI, S., T. HOGETSU, AND N. HARA. 1988. Arrangement of cortical microtubules at the surface of the shoot apex in *Vinca major* L.: observations by immunofluorescence microscopy. *Botanical Magazine, Tokyo* 101: 497–508.
- SCHWABE, W. W. 1984. Phyllotaxis. In P. W. Barlow and D. J. Carr [eds.], Positional controls in plant development, 403–440. Cambridge University Press, Cambridge.
- SELKER, J. L., AND P. B. GREEN. 1984. Organogenesis in *Graptopetalum paraguayense* E. Walther: shifts in orientation of cortical microtubule arrays are associated with periclinal divisions. *Planta* 160: 289–297.
- , AND R. F. LYNDON. 1996. Leaf initiation and de novo pattern formation in the absence of an apical meristem and pre-existing patterned leaves in the watercress (*Nasturtium officinale*) axillary explants. *Canadian Journal of Botany* 74: 625–641.
- SINNOTT, E. W., AND R. BLOCK. 1945. The cytoplasmic basis of intercellular patterns in vascular differentiation. *American Journal of Botany* 32: 151–156.
- SMITH, L. G., S. HAKE, AND A. W. SYLVESTER. 1996. The *tangle1* mutation alters cell division orientations throughout maize leaf development without altering leaf shape. *Development* 122: 481–489.
- SNOW, M., AND R. SNOW. 1935. Experiments on phyllotaxis III. Diagonal slits through decussate apices. *Philosophical Transactions of the Royal Society of London* B225: 63–94.
- STEINBERG, M. S., AND T. J. POOLE. 1981. Strategies for specifying form and pattern: adhesion-guided multicellular assembly. *Philosophical Transactions of the Royal Society of London* B295: 451–460.
- SYLVESTER, A. W., L. SMITH, AND M. FREELING. 1996. Acquisition of identity in the developing leaf. *Annual Review of Cell and Developmental Biology* 12: 257–304.
- SZILARD, R. 1974. Theory and analysis of plates, classical and numerical methods. Prentice Hall, Englewood Cliffs, NJ.
- TARNAI, T., AND Z. GASPÁR. 1995. Packing of equal circles in a square. *Acta Technica* 107: 123.
- THEIßEN, G., AND H. SAEDLER. 1995. MADS-box genes in plant ontogeny and phylogeny: Haeckel's 'biogenetic law' revisited. *Current Opinion in Genetics and Development* 5: 628–639.
- THOMPSON, D'ARCY W. 1942. On growth and form. Cambridge University Press, Cambridge.
- TIWARI, S. C., AND P. B. GREEN. 1991. Shoot initiation on a *Graptopetalum* leaf: sequential scanning electron microscopic analysis for epidermal division patterns and quantitation of surface growth (kinematics). *Canadian Journal of Botany* 69: 2302–2319.
- TURING, A. M. 1952. The chemical basis for morphogenesis. *Philosophical Transactions of the Royal Society of London* B237: 37–72.
- VAN ITERSON, G. 1907. Mathematische und mikroskopisch-anatomische Studien über Blattstellungen, nebst Betrachtungen über den Schalenbau der Miliolinien. Gustav Fischer Verlag, Jena.
- VEEN, A. H., AND A. LINDENMAYER. 1977. Diffusion mechanism for phyllotaxis. *Plant Physiology* 60: 127–139.
- WASTENEYS, G. O., AND R. E. WILLIAMSON. 1989. Reassembly of microtubules in *Nitella tasmanica*: quantitative analysis of assembly and orientation. *European Journal of Cell Biology* 50: 76–83.
- WIGGLESWORTH, V. B. 1940. Local and general factors in the development of "pattern" in *Rhodnius proxilus* (Hemiptera). *Journal of Experimental Biology* 17: 180–200.
- WILLIAMS, M. H. 1991. A sequential study of cell divisions and expansion patterns on a single developing shoot apex of *Vinca major*. *Annals of Botany* 68: 541–546.
- WILLIAMSON, R. E. 1991. Orientation of cortical microtubules in interphase plant cells. *International Review of Cytology* 129: 135–205.
- YOUNG, D. A. 1978. On the diffusion theory of phyllotaxis. *Journal of Theoretical Biology* 71: 421–432.



Paul B. Green (1931–1998)